Environ. Sci. Technol. **2007**, *41,* 5284−5290

Effect of Natural Organic Matter on Zinc Inhibition of Hematite Bioreduction by *Shewanella putrefaciens* CN32

JAMES J. STONE,*,† RICHARD A. ROYER,‡ BRIAN A. DEMPSEY,§ AND WILLIAM D. BURGOS§

Department of Civil and Environmental Engineering, South Dakota School of Mines and Technology, 501 East Saint Joseph Street, Rapid City, South Dakota 57701, Environmental Technology Laboratory, General Electric Company, One Research Circle, K1 4A12, Niskayuna, New York 12309, and Department of Civil and Environmental Engineering, The Pennsylvania State University, 212 Sackett Building, University Park, Pennsylvania 16802

The effect of zinc on the biological reduction of hematite (α-Fe_2O_3) by the dissimilatory metal-reducing bacterium (DMRB) *Shewanella putrefaciens* CN32 was studied in the presence of four natural organic materials (NOMs). Experiments were performed under non-growth conditions with H_2 as the electron donor and zinc inhibition was quantified as the decrease in the 5 d extent of hematite bioreduction as compared to no-zinc controls. Every NOM was shown to significantly increase zinc inhibition during hematite bioreduction. NOMs were shown to alter the distribution of both biogenic Fe(II) and Zn(II) between partitioned (hematite and cell surfaces) and solution phases. To further evaluate the mechanism(s) of NOM-promoted zinc inhibition, similar bioreduction experiments were conducted with nitrate as a soluble electron acceptor, and hematite bioreduction experiments were conducted with manganese which was essentially non-inhibitory in the absence of NOM. The results suggest that Me(II)−NOM complexes may be specifically inhibitory during solid-phase bioreduction via interference of DMRB attachment to hematite through the formation of ternary Me(II)−NOM−hematite complexes.

Introduction

Biological iron(III) reduction can be used to produce Fe(II)-rich reactive zones for the in situ treatment of contaminated groundwater. Iron(III) reduction can be stimulated by the addition of excess electron donor (e.g., lactate, acetate, ethanol) to promote the development of anaerobic conditions in a targeted subsurface location (*1*, *2*). Additional amendments to promote iron(III) reduction could include macro- and micronutrients and, possibly, natural organic materials (NOM). NOM addition may be considered because these materials have been shown to stimulate the bioreduction of solid-phase iron (hydr)oxides (*3*, *4*). Considering that NOM is known to complex metals (*5*−*9*), NOM addition could also conceivably decrease the toxicity of any metal co-contaminants.

The overarching premise of this study was to elucidate how NOM influences the inhibitory effects of heavy metal co-contaminants during biological iron(III) reduction. Zinc was selected for study because it is a common groundwater contaminant at U.S. Department of Energy facilities (*10*). A series of related studies have been conducted to examine the effect of zinc on the facultative dissimilatory metal-reducing bacterium (DMRB) *Shewanella putrefaciens* strain CN32. In one study, we showed that *S. putrefaciens* CN32 exhibited greater tolerance to zinc during solid-phase hematite reduction as compared to nitrate or oxygen reduction (*11*). We speculated that cells in biofilms on hematite surfaces could have developed greater resistance to zinc compared to freely dispersed cells. In the second study, we showed that amendments known to stimulate hematite reduction [anthraquinone-2,6-disulfonate (AQDS) and ferrozine] increased zinc toxicity (*12*). Mechanistic interpretations of these types of experiments are difficult because multiple factors (e.g., competitive Me(II) sorption, cell lethality) can exert either stimulation or inhibition effects at the same time. However, we concluded that metal toxicity was more important than metal sorption in inhibiting hematite reduction.

Building on these studies, the purpose of this research was to investigate the combined effects of zinc and NOM on the biological reduction of hematite by *Shewanella putrefaciens* CN32. Due to the ability of NOM to react with both solid phases and soluble species, NOM could impact Me(II)-promoted inhibition of solid-phase bioreduction through a variety of mechanisms. For example, NOM complexation with Me(II) would reduce the "free" metal activity (i.e., Me^{2+}) in solution, leading to a reduction in overall microbial Me(II) toxicity. Reduction of free metal activity has been previously demonstrated using synthetic metal chelating compounds such as EDTA and NTA (*13*, *14*). In addition, NOM may complex biogenic Fe(II), thereby enhancing solid-phase bioreduction through the prevention of surface passivation (*4*). Similar enhancement has been observed through the use of EDTA and NTA (*15*−*17*). To better differentiate these possible effects, similar experiments were conducted using nitrate to compare the systemic effect of zinc and NOM using a soluble electron acceptor in lieu of solid-phase hematite, and with a system containing hematite, NOM, and manganese to compare the inhibitory effects using a nontoxic Me(II), manganese.

Experimental Section

Materials. Hematite powder was obtained from J.T. Baker (Phillipsburg, NJ) and heated to 550 °C in air overnight before use to remove any residual organic carbon. The four NOMs tested from the International Humic Substances Society (IHSS) included the following: soil humic acid (SHA), Suwannee River humic acid (SRHA), Suwannee River fulvic acid (SRFA), and Suwannee River NOM (SRNOM). NOM suspensions dissolved in anaerobic 10 mM PIPES were added to each master reactor at the appropriate concentration. Aromaticity values for the NOMs were determined from ^{13}C NMR spectra from a published report for the IHSS materials (*18*). Proton titration data for all materials were used to determine NOM acidity (*19*). Characteristics of the NOM materials are provided in Table 1.

Bacterial Inoculum. *Shewanella putrefaciens* CN32 was grown aerobically on tryptic soy broth without dextrose (TSB-

* Corresponding author phone: 605-394-2443; fax: 605-394-5171; e-mail: James.Stone@sdsmt.edu.
† South Dakota School of Mines and Technology.
‡ General Electric Company.
§ The Pennsylvania State University.

10.1021/es062802l CCC: $37.00
Published on Web 06/23/2007

TABLE 1. Characteristics of IHSS Natural Organic Materials Used in Current Study

NOM	source	organic radical content[a] [spins $g^{-1} \times 10^{17}$]	acidity at pH 6.8[b] [meq g^{-1}]	Me(II) complexation capacity[c] [mM Me(II) g^{-1}]	aromaticity [%][d]	C content [%][a]	O/C ratio[a]
Soil HA	terrestrial	12.9	4.03	2.02	50	58.1	0.586
Suwannee River HA	aquatic	1.15	3.97	1.99	37	52.6	0.809
Suwannee River FA	aquatic	0.54	5.55	2.78	24	53.0	0.828
Suwannee River NOM	aquatic	0.54	4.08	2.04	24	48.8	0.814

[a] From IHSS Standard and Reference Collection. [b] From proton titrations in 0.01 M NaCl provided by Ritchie and Perdue (*19*). [c] Me(II) complexation capacity calculated by assuming 1 mol of Me(II) consumes 2 equiv of NOM acidity (*33*). Suwannee River NOM−Zn(II) complexation capacity was confirmed using 500 MWCO dialysis separation (Supporting Information Figure S1). [d] From Thorn et al. (*18*).

D) at 20 °C. Cells were harvested by centrifugation (4900*g*, 10 min, 20 °C) from a 16-hour-old culture (late log phase). The cells were washed three times in 10 mM 1,4-piperazinediethanosulfonic acid (PIPES; pH 6.8) buffer with the final wash made with deoxygenated buffer to remove residual oxygen. Cell density was determined by absorbance at 420 nm.

Bioreduction Experiment Preparation. A "master reactor" approach was used to prepare all experiments to ensure consistent chemical and biological conditions (*4*, *11*, *12*). All preparations were performed within a Coy anaerobic chamber (Grass Lakes, MI). The reactor was prepared by combining the electron acceptor and the bacterial inoculum in a 250 mL serum bottle. All solutions (except the zinc and manganese stocks) were prepared in 10 mM PIPES (pH 6.8). Before any NOM or metal addition to the master reactor, biotic no-NOM no-metal controls were prepared (in triplicate) by transferring 10 mL of the suspension into 20 mL amber serum bottles. The NOM was added before any metal to ensure that biotic with-NOM no-metal controls were prepared (in triplicate). Zinc or manganese was then incrementally added to the master reactor in an acidified, deoxygenated $ZnCl_2$ or $MnCl_2$ solution (1000 mg L^{-1} AAS certified standards) along with an equal volume of 0.1 N NaOH (for pH maintenance). At each concentration, 10 mL of the suspension was transferred into 20 mL amber serum bottles (in triplicate for zinc, duplicate for manganese). All serum bottles were sealed with Teflon-faced butyl rubber septa and aluminum crimp tops, and incubated outside the chamber in the dark at 20 °C on orbital shakers. Hydrogen from the anaerobic chamber atmosphere (97.5:2.5% N_2/H_2) was used as the electron donor in all experiments. The pH of the experiments never varied outside the range of 6.6−7.0.

Hematite Bioreduction. Experiments were performed with 2.0 g L^{-1} hematite (0.0125 mol Fe_2O_3 L^{-1}), a final cell density of 10^8 cells mL^{-1}, metal concentrations ranging from 0.02 to 0.23 mM total zinc or 0.02 to 1.82 mM total manganese, and the appropriate NOM (dissolved in 10 mM PIPES and added volumetrically). After 5 d incubation, reactors were sacrificed to measure dissolved and 0.5 N HCl extractable (total) Fe(II), dissolved and total metal, and pH.

Me(II) Distribution. Metal distribution results were determined using hematite bioreduction data described above. Partitioned Me(II) concentrations were operationally defined and calculated as the difference between the 0.5 N HCl extractable (total) and dissolved (both passing through 0.2 μm filter) metal concentrations, and are reported as mmoles of Me(II) per m^2 total sorbent surface area. Sorbent concentrations were 2.0 g L^{-1} hematite and 0.064 g L^{-1} cells, with cell mass estimated using an average cell weight of 6.4×10^{-10} mg dry wt. $cell^{-1}$ (*20*) and surface area of 140 m^2 g^{-1} (*21*, *22*) for *S. putrefaciens* CN32. Hematite surface area was 9.04 m^2 g^{-1} as measured by N_2-BET (*23*)

Analytical Techniques. Fe(II) was reported as dissolved, total, and partitioned. For dissolved Fe(II), samples were filtered (0.2 μm cellulose acetate), combined with ferrozine (1.96 mM ferrozine in 50 mM HEPES, pH 8.0) inside the chamber, and Fe(II) was measured by ferrozine outside the chamber (*24*). Solution pH of the filtrate was determined in the anaerobic chamber using a combination pH electrode. For total Fe(II), an unfiltered sample was acidified with HCl to achieve a final solution normality of 0.5 N. The solution was mixed for ca. 24 h, filtered (0.2 μm), and Fe(II) in the filtrate was measured by ferrozine (*24*). Dissolved and total metal were measured from the corresponding dissolved and total Fe(II) filtrate samples by flame atomic absorption spectrometry (AAS) after preservation with conc. HNO_3.

Data Analysis. Inhibition was defined as the percent change in bioreduction due to metal addition relative to its biotic no-metal control (*11*, *12*, *25*) and calculated as follows:

$$\%Inhibition = \left(1 - \frac{Bioreduction\ Extent\ with\ Me(II)}{Bioreduction\ Extent\ without\ Me(II)}\right) \times 100 \quad (1)$$

where the bioreduction extent was measured after 5 d for hematite reduction. It is important to note that for each series of experiments (with or without NOM), inhibition was calculated relative to its corresponding biotic no-metal control. The inhibitory concentration of metal required for 50% reduction in microbial metal reduction (IC_{50}) was calculated according to the following equation:

$$IC_{50} = 10^{\left(\frac{50-\beta_0}{\beta_1}\right)} \quad (2)$$

where β_0 was the *y*-axis intercept of the metal versus percent inhibition regression line and β_1 was the slope of the metal versus percent inhibition regression line, as adapted from the literature (*11*, *12*, *25*, *26*). Metal toxicity as determined by direct measurements of cell viability, e.g., by *Bac*light staining in our previous studies (*11*, *12*), was not possible in the presence of NOM due to interferences with *Bac*Light stain.

Results

Effect of Zinc and NOM on Hematite Bioreduction. Total Fe(II) (0.5 N HCl extractable) produced after 5 d as a function of zinc addition for varied concentrations of IHSS SHA (15−250 mg L^{-1}) and the with-SHA no-zinc controls are presented in Figure 1A. For each SHA concentration, biotic no-SHA no-zinc controls (results not shown) and biotic with-SHA no-zinc controls (data symbols on *y*-axis in Figure 1A) were also prepared. In the absence of zinc, all SHA concentrations ≥75 mg L^{-1} stimulated hematite bioreduction compared to their corresponding no-SHA controls. For example, 250 mg L^{-1} SHA stimulated Fe(II) production by 217% compared to its corresponding no-SHA control.

Low concentrations of zinc stimulated Fe(II) production in the presence (<150 mg L^{-1}) and absence of SHA (Figure 1A). Fe(II) production for the no-NOM control increased relative to its corresponding no-zinc control for

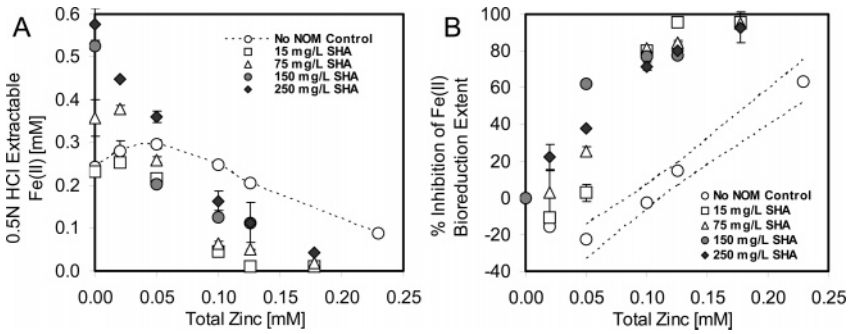

FIGURE 1. (A) 5 d 0.5 N HCl extractable Fe(II) production, and (B) inhibition of extent of hematite bioreduction as a function of total zinc for 15, 75, 150, 250 mg L^{-1} SHA and no-NOM control. Experiments performed using 2.0 g L^{-1} hematite, 10^8 cells mL^{-1} (*S. putrefaciens* CN32 under non-growth conditions) in 10 mM PIPES (pH 6.8). Values are mean of three replicates and error bars represent standard deviation (±standard deviation). Dashed lines (panel B) represent 95% confidence interval for total zinc ≥0.05 mM. Error bars smaller than symbol size not shown.

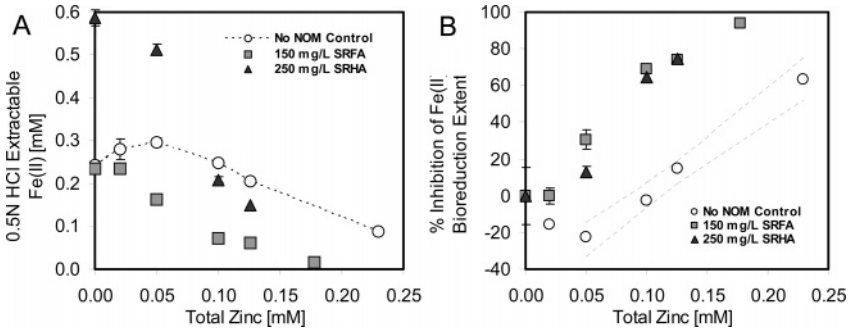

FIGURE 2. (A) 5 d 0.5 N HCl extractable Fe(II) production, and (B) inhibition of extent of hematite bioreduction as a function of total zinc for 150 mg L^{-1} SRFA, 250 mg L^{-1} SRHA, and no-NOM control. Experiments performed using 2.0 g L^{-1} hematite, 10^8 cells mL^{-1} (*S. putrefaciens* CN32 under non-growth conditions) in 10 mM PIPES (pH 6.8). Values are mean of three replicates and error bars represent standard deviation (±standard deviation). Dashed lines (panel B) represent 95% confidence interval. Error bars smaller than symbol size not shown.

total zinc concentrations up to 0.050 mM. Fe(II) production for 15 and 75 mg L^{-1} SHA increased for 0.020 mM total zinc addition relative to their no-zinc controls, and deceased for higher zinc concentrations. No stimulatory effect of zinc was observed for 150 and 250 mg L^{-1} SHA, where Fe(II) production steadily decreased with increasing zinc. Fe(II) production for the two lowest SHA concentrations and the no-NOM control conform to a Type II dose−response curve (stimulation followed by inhibition) as defined by Welp and Brummer (*27*). When applied to our system, maximum Fe(II) production occurred at low zinc concentrations, and decreased with increased zinc.

SHA addition resulted in increased zinc inhibition during hematite bioreduction (Figure 1B). The zinc concentration corresponding to a 50% decrease in the 5 d extent of hematite bioreduction compared to the no-zinc control was defined as the IC_{50}. The IC_{50} value was calculated from the total zinc concentration-vs-linear percent inhibition regression line developed. The IC_{50} value was 0.20 mM total zinc for the no-NOM control (open circles in Figure 1B). The addition of 15 mg L^{-1} SHA lowered the IC_{50} value to 0.078 mM total zinc, while increasing the SHA dose to 250 mg L^{-1} further reduced the IC_{50} to 0.056 mM total zinc. The general trend showed increasing SHA addition increased the inhibitory effect of zinc (i.e., decreased IC_{50} values) compared to the no-NOM controls. All concentrations of NOM decreased the zinc IC_{50} values between 60 and 88% compared to the no-NOM control. IC_{50} values based upon free Zn^{2+} concentrations were not calculated because zinc−NOM thermodynamic complexation constants were not available, and thus only IC_{50} values of total zinc have been reported.

The addition of IHSS SRFA (150 mg L^{-1}) and SRHA (250 mg L^{-1}) also increased zinc inhibition during hematite bioreduction (Figure 2). In the absence of zinc, 150 mg L^{-1} SRFA did not appreciably change Fe(II) production, while 250 mg L^{-1} SRHA increased Fe(II) production by 165% compared to their corresponding no-NOM controls. For SRFA and SRHA, little to no stimulatory effect of zinc was observed. The IC_{50} values for SRFA and SRHA were 0.068 and 0.085 mM total zinc, respectively. A summary of all zinc IC_{50} values determined during hematite bioreduction for the various NOMs studied is presented in Table 2.

Effect of Manganese and NOM on Hematite Bioreduction. Hematite bioreduction experiments using manganese instead of zinc were performed to determine whether Mn(II), having similar charge, molecular weight, and radius of hydration as Zn(II), inhibits hematite bioreduction similar to zinc. The manganese experiments were performed with 250 mg L^{-1} SHA and 150 mg L^{-1} SRFA, both previously shown to increase zinc inhibition during hematite bioreduction (Figures 1 and 2). Manganese did not inhibit hematite bioreduction in the absence of NOM (open circles in Figure 3) except at the highest concentration studied (1.82 mM). The IC_{50} value was 3.06 mM total manganese for the no-NOM control (open circles in Figure 3) (*12*). However, SRFA and SHA addition resulted in manganese inhibition, similar to the effects observed with zinc. The addition of 150 mg L^{-1} SRFA resulted in an IC_{50} of 0.16 mM total manganese, while 250 mg L^{-1} SHA resulted in IC_{50} of 0.85 mM total manganese (Table 3). Both IC_{50} concentrations for manganese were significantly higher (ca. > 2−10×) than those observed for zinc (i.e., manganese was less inhibitory than zinc).

Effect of NOM on Me(II) Distribution. The distribution of the divalent metals Fe(II), Zn(II), and Mn(II) between the solid (hematite and cell surfaces) and solution phases is important for interpreting the results from these experiments. Me(II) inhibition of hematite reduction could be caused by

TABLE 2. Summary of Zinc IC_{50}[a] Values, Partitioning Effects of NOMs, and Estimated NOM−Zn(II) Complexation Capacities Observed during the Biological Reduction of Hematite by *S. putrefaciens* CN32

NOM addition	total zinc IC_{50} (mM)	effect on Fe(II) partitioning[b]	effect on Zn(II) partitioning[b]	NOM−Me(II) complexation capacity (mM)[c]	total Me(II) (mM)[d]
15 mg L^{-1} SHA	0.078	+	+	0.030	0.14−0.27
75 mg L^{-1} SHA	0.063	+	+	0.15	0.16−0.40
150 mg L^{-1} SHA	0.025	+	var	0.30	0.23−0.25
250 mg L^{-1} SHA	0.056	var (−)	−	0.50	0.22−0.47
150 mg L^{-1} SRFA	0.069	0	var	0.42	0.17−0.25
250 mg L^{-1} SRHA	0.085	0	−	0.50	0.27−0.56

[a] Defined as inhibitory concentration of Zn(II) that caused 50% decrease in 5 d extent of hematite bioreduction compared to with-NOM no-Zn(II) control (*25*). IC_{50} value for no-NOM with-Zn(II) was 0.20 mM total zinc (*11*). [b] Symbols: (+) always increased partitioning, (−) always decreased partitioning, (var) increased and decreased partitioning, (0) partitioning unchanged. [c] Calculated from NOM acidity at pH 6.8 in 0.01 M NaCl solution (*19*) assuming 1 mol Me(II) consumes 2 equiv of acidity (*33*). [d] Calculated as total biogenic Fe(II) produced + total Zn(II) added.

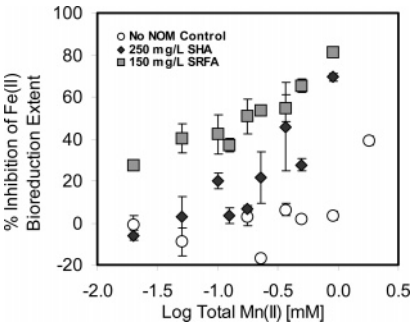

FIGURE 3. Inhibition of extent of hematite bioreduction as a function of total manganese for 250 mg L^{-1} SHA, 150 mg L^{-1} SRFA, and no-NOM control. Experiments performed using 2.0 g L^{-1} hematite, 10^8 cells mL^{-1} (*S. putrefaciens* CN32 under non-growth conditions) in 10 mM PIPES (pH 6.8). Values are mean of two replicates and error bars represent standard deviation (±standard deviation). Error bars smaller than symbol size not shown.

either Me(II) toxicity leading to cell death or Me(II) and/or NOM partitioning leading to hematite surface blockage, or a combination of both. Divalent metal partitioning was calculated as the difference between the total and dissolved Me(II) measurements during the hematite bioreduction experiments. Freundlich isotherms were chosen to model the distribution of Fe(II) between solid (hematite and cell surfaces) and solution phases because they consistently provided greater correlation coefficients compared to Langmuir isotherms. For consistency, Freundlich isotherms were also used to model zinc and manganese distributions. Interpretation of these distribution results may be limited due to variable biogeochemical differences associated with the batch systems (e.g., competitive Me(II) partitioning, potential for biomineralization, variable Fe(II) production), however, Me(II) distributions provide critical information regarding bioreduction system behavior.

The effect of NOM on the distribution of Fe(II) during hematite bioreduction (in the absence of zinc) is presented in Figure 4A. The Fe(II) partitioning measurements (data points in Figure 4A) were calculated from 5 d hematite bioreduction experiments amended with the specified NOM concentration (i.e., from biotic with-NOM, no-zinc controls). Fe(II) partitioning increased (greater than 95% confidence interval) for the three lowest SHA concentrations (15, 75, and 150 mg L^{-1} SHA) tested, while SHFA and SRHA did not alter Fe(II) partitioning. SHA, collected from a terrestrial environment, exhibited greater aromaticity (Table 1) and is presumably more hydrophobic in nature compared to the aquatic Suwannee River materials. These characteristics, as compared to SRFA and SRHA, may affect solid- and solution-phase distribution, thus potentially altering overall Me(II) distribution. Suwannee River NOM−Zn(II) complexation capacity was confirmed using 500 MWCO dialysis separation (Supporting Information Figure S1).

The effect of NOM with-zinc on the distribution of Fe(II) during hematite bioreduction is presented in Figure 4B. A second "baseline" Fe(II) partitioning isotherm (solid line in Figure 4B) was developed from a series of no-NOM with-zinc controls (containing 0.020−0.23 mM total zinc). The Fe(II) partitioning measurements (data points in Figure 4B) were calculated from 5 d hematite bioreduction experiments amended with the specified NOM concentration and variable zinc concentrations. For each data set, the highest dissolved Fe(II) concentrations correspond to the lowest zinc concentrations tested for each NOM tested since increased zinc addition typically resulted in less Fe(II) production (Figure 1). Fe(II) partitioning generally increased with increased SHA addition (Table 2), with the exception of 250 mg L^{-1} SHA where Fe(II) partitioning decreased or did not change. SRHA had no significant effect on Fe(II) distribution, while SRFA increased Fe(II) only for dissolved Fe(II) concentrations greater than 0.084 mM (measured for 0.05 mM total zinc addition).

The effect of NOM on the distribution of zinc during hematite bioreduction [in the presence of 0.012 to 0.51 mM biogenic Fe(II)] is presented in Figure 4C. A "baseline" Zn-(II)-in-the-presence-of-Fe(II) partitioning isotherm (solid line in Figure 4C) was developed from the same no-NOM with-zinc controls (0.020−0.23 mM total zinc). The zinc partitioning measurements (data points in Figure 4C) were calculated from 5 d hematite bioreduction experiments amended with the specified NOM concentration and variable zinc concentrations. Results from Figure 4C indicate that NOM did not systematically effect zinc partitioning, unlike the relatively consistent increase (or no change) observed for Fe(II) partitioning (Figure 4B, Table 2). SRFA (150 mg L^{-1}) and 150 mg L^{-1} SHA addition both increased or decreased zinc partitioning depending on the zinc concentration, while SRHA (250 mg L^{-1}) always decreased zinc partitioning. The two lowest SHA concentrations (15 and 75 mg L^{-1}) generally increased zinc partitioning, while 250 mg L^{-1} SHA always decreased zinc partitioning. As discussed in (*8*), these differences could be attributed to dissimilarities in competitive zinc partitioning in the presence of SHA, or changes in the solubility of the zinc−humic acid complexes relative to SHA concentrations. Results are summarized in Table 2.

The effect of NOM with-manganese on the distribution of Mn(II) during hematite bioreduction is presented in Figure 4D. The solid line represents a "baseline" Mn(II)-in-the-presence-of-Fe(II) [ca. 0.060 to 0.71 mM biogenic Fe(II)] partitioning isotherm developed from a series of no-NOM with-manganese controls (0.020−1.8 mM manganese). Mn(II) partitioning measurements (i.e., data points in Figure 4D) were calculated from 5 d hematite bioreduction

TABLE 3. Summary of Manganese IC_{50}[a] Values, Partitioning Effects of NOMs, and NOM−Mn(II) Complexation Capacities during the Biological Reduction of Hematite by *S. putrefaciens* CN32

NOM addition	total manganese IC_{50} (mM)[b]	effect on Mn(II) partitioning[c]	NOM−Me(II) complexation capacity (mM)[d]	total Me(II) (mM)[e]
250 mg L^{-1} SHA	0.85	+	0.50	0.64−1.1
150 mg L^{-1} SRFA	0.16	var	0.42	0.24−0.97

[a] Defined as inhibitory concentration of Mn(II) that caused 50% decrease in 5 d extent of hematite bioreduction compared to with-NOM no-Mn(II) control (*25*). IC_{50} value for no-NOM with-Mn(II) was 3.06 mM total manganese (*12*). [b] IC_{50} values were calculated from the least-squares lines obtained from the data presented in Figure 3. [c] Symbols: (+) always increased partitioning, (−) always decreased partitioning, (var) increased and decreased partitioning, (0) partitioning unchanged. [d] Calculated from NOM acidity at pH 6.8 in 0.01 M NaCl solution assuming 1 mol Me(II) can consume 2 equiv of acidity (*33*). [e] Calculated as total biogenic Fe(II) produced + total Mn(II) added.

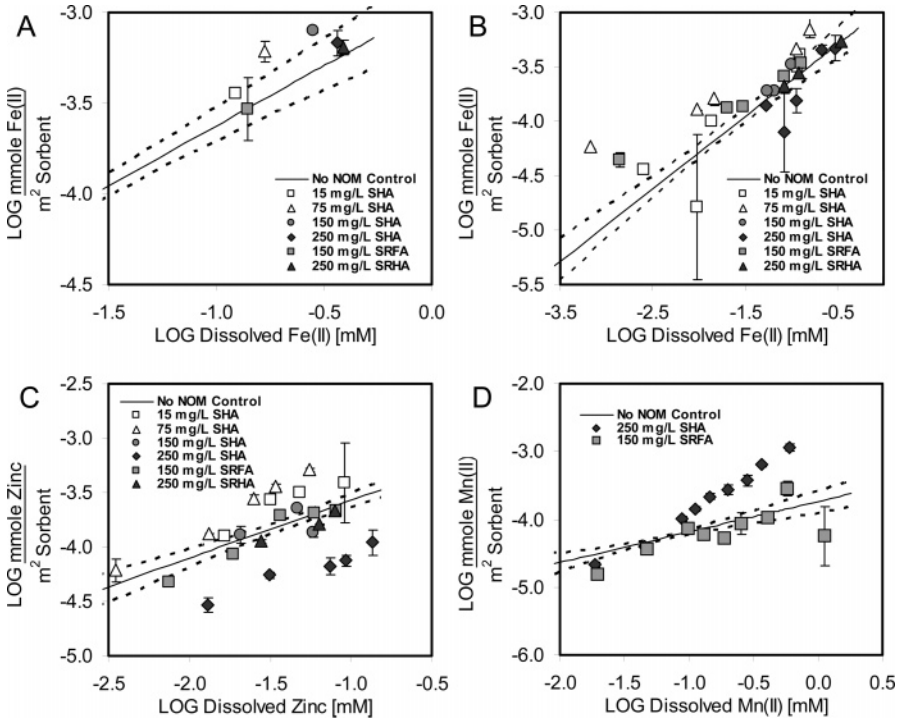

FIGURE 4. Distribution of (A) Fe(II) in the absence of zinc, and (B) Fe(II) in the presence of zinc (0.020−0.23 mM), (C) zinc in the presence of Fe(II) (0.012−0.51 mM), and (D) manganese in the presence of Fe(II) (0.060−0.71 mM) as a function of NOM during hematite bioreduction. Solid lines represent Freundlich isotherms for no-NOM, with Me(II) controls and dashed line represents 95% confidence intervals. Experiments performed using 2.0 g L^{-1} hematite, 10^8 cells mL^{-1} (*S. putrefaciens* CN32 under non-growth conditions) in 10 mM PIPES (pH 6.8). Values are mean of three replicates and error bars represent standard deviation (±standard deviation). Error bars smaller than symbol size not shown.

experiments with the specified NOM concentration and variable manganese concentrations. SHA addition increased Mn(II) partitioning at dissolved Mn(II) concentrations greater than 0.045 mM, while SRFA addition did not alter Mn(II) partitioning (Table 3).

Discussion

Results from this study demonstrate that all NOMs significantly increased zinc inhibition during hematite bioreduction, however, not all NOM addition resulted in increased zinc partitioning (Table 2). For example, SRFA did not effect Fe(II) partitioning except at very low dissolved Fe(II) concentrations (<0.03 mM; Figure 4A and B) and had little effect on Zn(II) (Figure 4C) or Mn(II) partitioning (Figure 4D), yet significantly increased both zinc and manganese inhibition of hematite bioreduction (Figures 2B and 3). As expected, Me(II)−NOM complexes did not inhibit nitrate bioreduction (using Zn(II); Supporting Information Figure S2), thus interactions between Me(II) and NOM in the absence of a solid-phase electron acceptor decreased inhibition. Surprisingly, NOM addition resulted in manganese inhibition when, in the absence of NOM, manganese did not inhibit bioreduction (Figure 3). Increased Me(II) partitioning cannot be the sole cause of NOM-promoted Me(II) inhibition because inhibition occurred with or without increased Me(II) partitioning. These results warrant further analysis regarding how Me(II)−NOM complexes specifically interfere with hematite bioreduction.

Our interpretation of these results suggests that the formation of hematite−Me(II)−NOM or cell−Me(II)−NOM complexes, or "ternary surface complexes" (*28*) either partitioned (to hematite and/or cell surfaces) or in solution, could be responsible for the inhibition effects observed. The formation of a ternary Me(II)−SHA−hematite surface complex has been described by Murphy et al. (*28*) where free metals are bound between hematite surface hydroxyls and ionized functional groups of NOM. While our operational definition of partitioned Me(II) concentration does not distinguish between the distribution of Me(II) to hematite or cells, or between the distribution of Me(II) or Me(II)−NOM complexes to these surfaces, we speculate that the preferential partitioning of Me(II)−NOM complexes (i.e., the formation

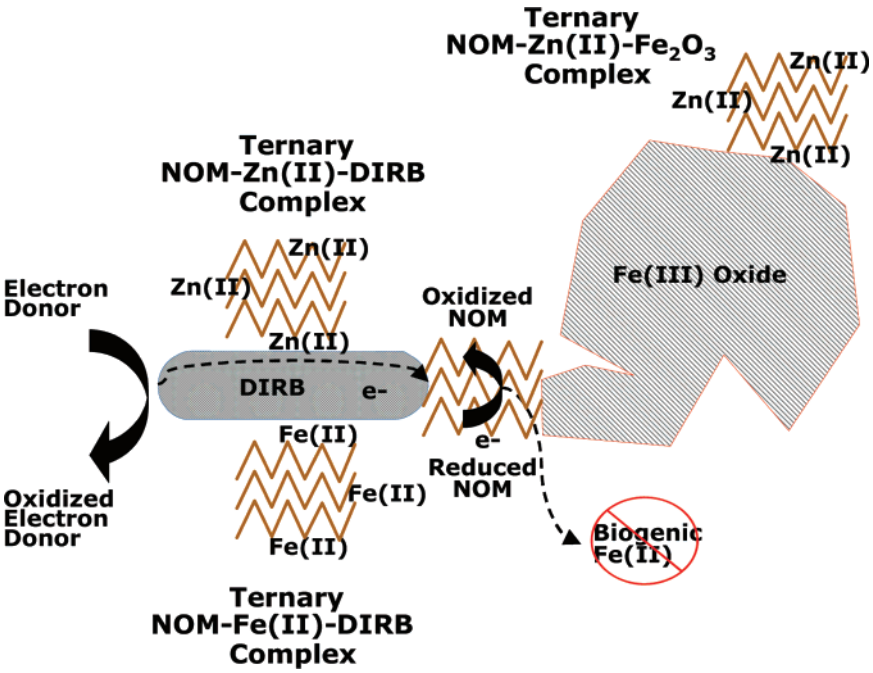

FIGURE 5. Conceptualization of important reactive species during hematite bioreduction by DMRB in presence of NOM, as adapted from Royer et al. (*4*).

of ternary Me(II)−NOM−hematite and/or Me(II)−NOM−cell complexes) compared to Me(II) could magnify the inhibitory effect of these complexes. It is also possible that the partitioning of Me(II)−NOM complexes increased even under conditions when operationally defined Me(II) partitioning decreased. We speculate that the mechanism of NOM-promoted Me(II) inhibition of hematite bioreduction could be interference in attachment of DMRB to hematite due to Me(II)−NOM complexes partitioned to either DMRB or hematite, as shown in Figure 5.

Nitrate bioreduction experiments (Supporting Information Figure S2) clearly showed that Me(II)−NOM complexes were not inhibitory to *S. putrefaciens* CN32. Dialysis experiments confirmed that Zn(II)−NOM complexes did form under this solution chemistry (Supporting Information Figure S1). Furthermore, because *S. putrefaciens* CN32 was the sole sorbent in the nitrate bioreduction experiments, Me(II)−NOM−DMRB ternary complexes (if formed) were also not inhibitory to *S. putrefaciens* CN32. Instead, the nitrate reduction results suggest that NOM acted as an effective scavenger or complexing agent for minimizing bioavailable free Zn^{2+}. This was not the case during solid-phase hematite reduction. While one would assume that NOM was again effective at complexing free zinc, Zn(II)−NOM complexes appeared to instead passify the hematite surface, and subsequently increased the overall inhibitory effect of zinc during hematite bioreduction. Results from this study suggest that these ternary Me(II)−NOM−hematite complexes formed at the hematite surface passivate the surface and decrease the bioavailability of surface Fe(III).

The enhancement of dissimilatory iron(III) reduction through the addition of NOM and supplemental electron donors and nutrients has been thought of as a viable environmental remediation tool for *in situ* heavy metal and radionuclide contaminant cleanup. The applicability of biologically mediating reducible metals [e.g., Cr(VI)] and radionuclides [e.g., Tc(VII), U(VI)] has been proven under both laboratory and field settings (*29*−*32*), however, results from this study suggest that ancillary reactions between NOM with other metal co-contaminants should be considered when evaluating bioremediation applicability.

Acknowledgments

Research supported by the Natural and Accelerated Bioremediation Research Program (NABIR), Office of Biological and Environmental Research (OBER), Office of Energy Research, U.S. Department of Energy (DOE), grant DE-FG02-01ER63180 is gratefully acknowledged. J.J.S. acknowledges support from National Science Foundation/EPSCoR Grant EPS-0091948, and the State of South Dakota Governor's 2010 Seed Grant program.

Supporting Information Available

Equilibrium dialysis and nitrate bioreduction results. This material is available free of charge via the Internet at http://pubs.acs.org.

Literature Cited

(1) Lovley, D. R.; Phillips, E. J. P. Organic matter mineralization with reduction of ferric iron in anaerobic sediments. *Appl. Environ. Microbiol.* **1986**, *51*, 683−689.
(2) Lovley, D. R.; Phillips, E. J. P.; Lonergan, D. J. Hydrogen and formate oxidation coupled to dissimilatory reduction of iron or manganese by *Alteromonas putrefaciens*. *Appl. Environ. Microbiol.* **1989**, *55*, 700−706.
(3) Chen, J.; Gu, B. H.; Royer, R. A.; Burgos, W. D. The roles of natural organic matter in chemical and microbial reduction of ferric iron. *Sci. Total Environ.* **2003**, *307*, 167−178.
(4) Royer, R. A.; Burgos, W. D.; Fisher, A. S.; Jeon, B. H.; Unz, R. F.; Dempsey, B. A. Enhancement of hematite bioreduction by natural organic matter. *Environ. Sci. Technol.* **2002**, *36*, 2897−2904.
(5) Lenhart, J. J.; Cabaniss, S. E.; MacCarthy, P.; Honeyman, B. D. Uranium(VI) complexation with citric, humic and fulvic acids. *Radiochim. Acta* **2000**, *88*, 345−353.
(6) Dzombak, D. A.; Fish, W.; Morel, F. M. Metal−humate interactions. 1. Discrete ligand and continuous distribution models. *Environ. Sci. Technol.* **1986**, *20*, 669−675.
(7) Fish, W.; Dzombak, D. A.; Morel, F. M. Metal−humate interactions. 2. Application and comparison of models. *Environ. Sci. Technol.* **1986**, *20*, 676−683.
(8) Spark, K. M.; Wells, J. D.; Johnson, B. B. Sorption of heavy metals by mineral-humic acid substrates. *Aust. J. Soil. Res.* **1997**, *35*, 113−122.
(9) Redman, A. D.; Macalady, D. L.; Ahmann, D. Natural organic matter affects arsenic ppeciation and sorption onto hematite. *Environ. Sci. Technol.* **2002**, *36*, 2889−2896.

(10) Riley, R. G.; Zachara, J. M. Wobber, F. J., Eds. *Chemical Contaminants on DOE Lands and Selection of Contaminat Mixtures for Subsurface Science Research*; DOE/ER-0547T; U.S. Department of Energy: Washington, DC, 1992.
(11) Stone, J. J.; Burgos, W. D.; Royer, R. A.; Dempsey, B. A. Impact of zinc on biological Fe(III) and nitrate reduction by *Shewanella putrefaciens* CN32. *Environ. Eng. Sci.* **2006**, *23*, 691−704.
(12) Stone, J. J.; Burgos, W. D.; Royer, R. A.; Dempsey, B. A. Zinc and manganese inhibition of biological hematite reduction. *Environ. Eng. Sci.* **2006**, *23*, 859−870.
(13) Shuttleworth, K. L.; Unz, R. F. Influence of metals and metal speciation on the growth of filamentous bacteria. *Water Res.* **1991**, *25*, 1177−1186.
(14) Shuttleworth, K. L.; Unz, R. F. Sorption of heavy-metals to the filamentous bacterium Thiothrix strain A1. *Appl. Environ. Microbiol.* **1993**, *59*, 1274−1282.
(15) Roden, E. E.; Urrutia, M. M. Ferrous iron removal promotes microbial reduction of crystalline iron(III) oxides. *Environ. Sci. Technol.* **1999**, *33*, 1847−1853.
(16) Roden, E. E.; Urrutia, M. M. Influence of biogenic Fe(II) on bacterial crystalline Fe(III) oxide reduction. *Geomicrobiol. J.* **2002**, *19*, 209−251.
(17) Urrutia, M. M.; Roden, E. E.; Zachara, J. M. Influence of aqueous and solid-phase Fe(II) complexants on microbial reduction of crystalline iron(III) oxides. *Environ. Sci. Technol.* **1999**, *33*, 4022−4028.
(18) Thorn, K. A.; Folan, D. W.; MacCarthy, P. Characterization of the International Humic Substances Society standard and reference fulvic and humic acids by solution state carbon-13 (p13 sC) and hydrogen-1 (p1 sH) nuclear magnetic resonance spectrometry; USGS Water Resources Investigations Report 200; USGS: Reston, VA, 1989.
(19) Ritchie, J. M.; Perdue, E. M. E. Proton-binding study of standard and reference fulvic acids, humic acids, and natural organic matter. *Geochim. Cosmochim. Acta* **2003**, *67*, 85−96.
(20) Liu, C. X.; Zachara, J. M.; Fredrickson, J. K.; Kennedy, D. W.; Dohnalkova, A. Modeling the inhibition of the bacterial reduction of U(VI) by beta-$MnO_{2(S)(g)}$. *Environ. Sci. Technol.* **2002**, *36*, 1452−1459.
(21) Fein, J. B.; Daughney, C. J.; Yee, N.; Davis, T. A. A chemical equilibrium model for metal adsorption onto bacterial surfaces. *Geochim. Cosmochim. Acta* **1997**, *61*, 3319−3328.
(22) Sokolov, I.; Smith, D. S.; Henderson, G. S.; Gorby, Y. A.; Ferris, F. G. Cell surface electrochemical heterogeneity of the Fe(III)-reducing bacteria *Shewanella putrefaciens*. *Environ. Sci. Technol.* **2001**, *35*, 341−347.
(23) Jeon, B. H.; Dempsey, B. A.; Burgos, W. D.; Royer, R. A. Reactions of ferrous iron with hematite. *Colloids Surf., A* **2001**, *191*, 41−55.
(24) Stookey, L. L. Ferrozine - A new spectrophotometric reagent for iron. *Anal. Chem.* **1970**, *42*, 779−781.
(25) Sani, R. K.; Peyton, B. M.; Brown, L. T. Copper-induced inhibition of growth of *Desulfovibrio desulfuricans* G20: Assessment of its toxicity and correlation with those of zinc and lead. *Appl. Environ. Microbiol.* **2001**, *67*, 4765−4772.
(26) Ritchie, J. M.; Cresser, M.; Cotter-Howells, J. Toxicological response of a bioluminescent microbial assay to Zn, Pb and Cu in an artificial soil solution: relationship with total metal concentrations and free ion activities. *Environ. Pollut.* **2001**, *114*, 129−136.
(27) Welp, G.; Brummer, G. W. Microbial toxicity of Cd and Hg in different soils related to total and water-soluble contents. *Ecotoxicol. Environ. Safe.* **1997**, *38*, 200−204.
(28) Murphy, R. J.; Lenhart, J. J.; Honeyman, B. D. The sorption of thorium (IV) and uranium (VI) to hematite in the presence of natural organic matter. *Colloids Surf., A* **1999**, *157*, 47−62.
(29) Fendorf, S.; Wielinga, B. W.; Hansel, C. M. Chromium transformations in natural environments: The role of biological and abiological processes in Chromium(VI) reduction. *Intern. Geol. Rev.* **2000**, *42*, 691−701.
(30) Wildung, R. E.; Gorby, Y. A.; Krupka, K. M.; Hess, N. J.; Li, S. W.; Plymale, A. E.; McKinley, J. P.; Fredrickson, J. K. Effect of electron donor and solution chemistry on products of dissimilatory reduction of technetium by *Shewanella putrefaciens*. *Appl. Environ. Microbiol.* **2000**, *66*, 2451−2460.
(31) Liu, C.; Gorby, Y. A.; Zachara, J. M.; Fredrickson, J. K.; Brown, C. F. Reduction kinetics of Fe(III), Co(III), U(VI), Cr(VI), and Tc(VII) in cultures of dissimilatory metal-reducing bacteria. *Biotechnol. Bioeng.* **2002**, *80*, 637−649.
(32) Wielinga, B.; Mizuba, M. M.; Hansel, C. M.; Fendorf, S. Iron promoted reduction of chromate by dissimilatory iron-reducing bacteria. *Environ. Sci. Technol.* **2001**, *35*, 522−527.
(33) Stevenson, F. J. *Humus Chemistry: Genesis, Composition, Reactions,* 2nd ed.; John Wiley and Sons, Inc.: New York, 1994.

Received for review November 26, 2006. Revised manuscript received March 26, 2007. Accepted May 21, 2007.

ES062802L